

# Thermally assisted magnetization reversal of a magnetic nanoparticle driven by a down-chirp microwave field pulse

M. T. Islam<sup>a</sup>, M. A. J. Pikul<sup>a</sup> and X. S. Wang<sup>b,\*</sup>

<sup>a</sup>Physics Discipline, Khulna University, Khulna 9208, Bangladesh

<sup>b</sup>School of Physics and Electronics, Hunan University, Changsha 410082, China

## ARTICLE INFO

### Keywords:

Magnetization reversal  
Thermal effect  
sLLG equation  
Energy barrier  
Stability factor

## ABSTRACT

It has been shown that a single-domain magnetic nanoparticle can be effectively switched by a linear down-chirp microwave field pulse (DCMWP) in zero temperature limit. However, finite temperature is ubiquitous in practice. Here, we study the effect of finite temperature on the DCMWP-induced magnetization reversal based on the stochastic Landau-Lifshitz-Gilbert equation. It is found that any one of the three controlling parameters of a DCMWP, i.e. the amplitude, chirp rate, or initial frequency, decreases with increasing temperature while the other two are fixed. The maximal temperature at which the reversal can happen increases with enlarging the system size. These phenomena are related to the facts that the energy barrier induced by anisotropy increases with the system volume, and the effective magnetization decreases with temperature. We also provide a set of optimal parameters for practical realization of our proposal. These findings may provide a way to realize low-cost and fast magnetization reversal with a wide operating temperature.

## 1. Introduction

Fast and energy-efficient magnetization reversal of magnetic nanoparticle draws much attention because of its application in non-volatile data storage device [1, 2, 3] and rapid information processing [4]. For practical realization, a wide range of operating temperature is required which can be obtained by employing the high-anisotropy materials which belong to higher energy barrier [5]. But the challenging issue is to find out the way to achieve fast magnetization reversal for high-anisotropy materials with minimal energy. In the early years, magnetization reversal was induced by a constant magnetic field [6, 7] which requires the larger reversal time [6] and it suffers from scalability and field localization issue for nano-device. The spin-polarized electric current directly or indirectly becomes a potential candidate to induce magnetization reversal through spin transfer torque (STT) and/or spin orbit torque (SOT) [8, 9, 10, 11, 12, 13, 14, 15, 16, 17, 18, 19, 20, 21, 22]. However, in case of the STT-MRAM or SOT-MRAM based device fabrication, the requirement of a large current density is an obstacle since it generates Joule heat which limits the device durability and reliability [23, 24, 25, 26, 27, 28, 29]. Later on, people digress to utilize the microwave field of constant or time dependent frequency, either with or without a polarized electric current, to induce magnetization reversal [30, 31, 32, 33, 34, 35, 36, 37, 38, 39, 40, 41].


Recently, we proposed that a down-chirp microwave pulse (DCMWP) is capable of inducing subnanosecond magnetization reversal with proper initial frequency  $f_0$ , chirp rate  $\eta$  and field amplitude  $H_{\text{mw}}$  at 0 temperature [42]. However, finite temperature is ubiquitous in nature, and it is practi-

cally meaningful to study the effect of finite temperature on DCMWP-induced magnetization reversal. Indeed, the magnetization reversal is to overcome the energy barrier originated from the anisotropy, but the finite temperature provides an isotropic background energy which makes the reversal easier. There are several studies demonstrating the thermal effect assists magnetization reversal induced by magnetic field or electric current [43, 44, 45, 46, 47]. If the temperature is too high, there will be a significant probability that the magnetization reverses simultaneously, which is undesired. Therefore, it is meaningful to investigate how the optimal initial frequency, chirp rate and field amplitude change with temperature, and the allowed temperature interval for DCMWP-induced magnetization reversal. For device applications, the working temperature is usually the room temperature. So it is useful to check whether the DCMWP-driven magnetization reversal is still valid at room temperature. In this paper, we show that the thermal effect assists the DCMWP-induced magnetization reversal. Each of  $f_0$ ,  $\eta$  and  $H_{\text{mw}}$  decreases with increasing temperature while the other two are fixed, until a maximal temperature above which the reversal is no longer valid. The maximal temperature increases with enlarging the system size and hence a wide operating temperature above room temperature is possible. Therefore, these findings may provide a way to realize low-cost and fast magnetization reversal with a wide operating temperature.

## 2. Analytical model and method

We consider a single-domain ferromagnetic nanoparticle with uniaxial easy-axis anisotropy along  $z$  axis at finite temperature  $T$ , as shown in Fig. 1(a). The magnetization direction is represented by a unit vector  $\mathbf{m}$  with saturation magnetization  $M_s$ . When the nanoparticle is small, it can be regarded as a macrospin, as illustrated in the figure. Never-

\*Corresponding author:

 justicewxs@hnu.edu.cn (X.S. Wang)

ORCID(s): 0000-0002-3846-4009 (M.T. Islam); 0000-0002-7500-1572 (M.A.J. Pikul); 0000-0003-1374-4407 (X.S. Wang)

theless, we use smaller mesh size (from  $0.5 \text{ nm} \times 0.5 \text{ nm} \times 0.5 \text{ nm}$  to  $2 \text{ nm} \times 2 \text{ nm} \times 2 \text{ nm}$ , depending on the edge length) to mimic the realistic condition. The ground-state magnetization directions are all  $\mathbf{m}$  parallel to  $\hat{\mathbf{z}}$  and  $-\hat{\mathbf{z}}$ .

In the presence of a circularly polarized DCMWP and finite temperature, the magnetization dynamics is governed by the stochastic Landau Lifshitz Gilbert (sLLG) equation [48]

$$\frac{d\mathbf{m}}{dt} = -\gamma \mathbf{m} \times (\mathbf{H}_{\text{eff}} + \mathbf{h}_{\text{th}}) + \alpha \mathbf{m} \times \frac{\partial \mathbf{m}}{\partial t} \quad (1)$$

where  $\alpha$  and  $\gamma$  are the Gilbert damping constant and gyromagnetic ratio respectively, and the effective field ( $\mathbf{H}_{\text{eff}}$ ) comes from the microwave magnetic field  $\mathbf{H}_{\text{mw}}$ , the exchange field  $\frac{2A}{M_s} \nabla^2 \mathbf{m}$ , and the easy-axis anisotropy field along  $z$  direction  $\mathbf{H}_k = H_k m_z \hat{\mathbf{z}}$ .  $\mathbf{h}_{\text{th}}$  is the stochastic thermal field due to the finite temperature. The thermal field follows the Gaussian process characterized by following relations [49]

$$\begin{aligned} \langle h_{\text{th},ip}(t) \rangle &= 0, \\ \langle h_{\text{th},ip}(t) h_{\text{th},jq}(t + \Delta t) \rangle &= \frac{2\alpha k_B T}{\gamma M_s V} \delta_{ij} \delta_{pq} \delta(\Delta t), \end{aligned} \quad (2)$$

where  $\langle \rangle$  denotes the ensemble average,  $i$  and  $j$  label the micromagnetic cells,  $p$  and  $q$  represent the Cartesian components of the thermal field,  $V$  is the volume of one micromagnetic cell, and  $k_B$  is the Boltzman constant. Since we are considering a macrospin model,  $V$  is the volume of the whole particle.

In the absence of external force and at zero temperature, the magnetization of nanoparticle has two stable states  $\mathbf{m} \parallel \hat{\mathbf{z}}$  and  $\mathbf{m} \parallel -\hat{\mathbf{z}}$  due to the easy axis. To reverse the magnetization from one equilibrium state to the other, it is previously reported [42] that a circularly polarized DCMWP which takes the form  $\mathbf{H}_{\text{mw}} = H_{\text{mw}} [\cos \phi(t) \hat{\mathbf{x}} + \sin \phi(t) \hat{\mathbf{y}}]$  can induce fast reversal at zero temperature limit.  $\phi(t)$  is the phase giving the instantaneous frequency of DCMWP  $f(t) \equiv \frac{1}{2\pi} \frac{d\phi}{dt}$ , the frequency linearly decreases from  $f_0$  to  $-f_0$  with a chirp rate  $\eta$  (with unit of  $\text{ns}^{-2}$ ) as  $f = f_0 - \eta t$ , as shown in Fig. 1(b). The phase is thus  $\phi(t) = 2\pi(f_0 t - \frac{\eta}{2} t^2)$ , and the duration of the microwave pulse is  $\tau = \frac{2f_0}{\eta}$ . Subnanosecond magnetization reversal is achieved with the physical picture that the DCMWP triggers stimulated microwave absorptions (emissions) by (from) the spin before (after) it crosses over the energy barrier at  $T = 0$  [42].

In this study, the following parameters are selected from the representative experiments on microwave-driven magnetization reversal as  $M_s = 10^6 \text{ A/m}$ ,  $H_k = 0.75 \text{ T}$ ,  $\gamma = 1.76 \times 10^{11} \text{ rad/T/s}$ ,  $A = 13 \times 10^{-12} \text{ J/m}$ , and  $\alpha = 0.01$ . We use MuMax3 Package [50] to numerically solve stochastic LLG equation choosing adaptive Heun solver. To rule out the effect of shape anisotropy, we consider cubic nanoparticles with edge length  $a$  throughout this paper.  $a = 2, 4, 8, 12 \text{ nm}$  are studied. Considering the time-efficiency as well as stability [51], we use the time step of  $10^{-15} \text{ s}$  for small volume ( $2 \times 2 \times 2 \text{ nm}^3$ ), and  $10^{-14} \text{ s}$  for other larger volumes.

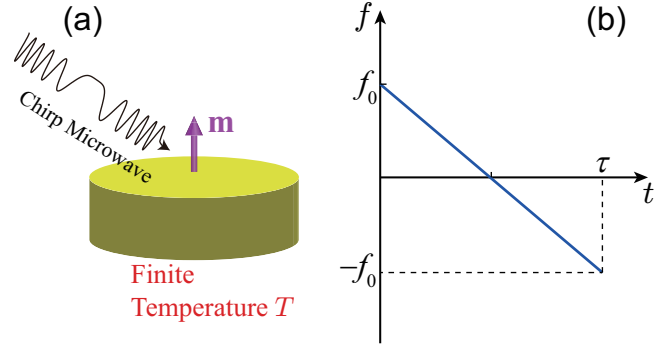


**Figure 1:** (a) Schematic diagram of the system. The magnetization  $\mathbf{m}$  is driven by a chirp microwave at finite temperature. A down-chirp microwave field is applied onto a nanoparticle at finite temperature. (b) The frequency profile (sweeping from  $+f_0$  to  $-f_0$ ) of a down-chirp microwave.

Each numerical result is obtained from the average of 12 random tests with different random seeds. We define the switching time as the time at which the magnetization reaches  $m_z = -0.7$ , considering practical requirement.

### 3. Numerical Results

We first focus on a  $4 \times 4 \times 4 \text{ nm}^3$  nanoparticle and study the effect of temperature on the DCMWP-driven magnetization reversal. We keep the initial frequency  $f_0 = 21 \text{ GHz}$ , and the microwave field  $H_{\text{mw}} = 0.045 \text{ T}$  (which are same as the zero-temperature parameters obtained in [42]) fixed, and try to find the optimal chirp rate  $\eta$  (i.e. the chirp rate that leads to fastest reversal). The zero-temperature optimal chirp rate  $\eta_0$  is  $67.2 \text{ ns}^{-2}$  according to [42]).

The temporal evolution of  $m_z$  at this optimal chirp rate and at  $0 \text{ K}$  is shown by the black line in Fig. 2(a). However, when the temperature becomes finite ( $T = 10 \text{ K}$ ), the same chirp rate can no longer drive the magnetization reversal, as shown by the red line. By tuning the chirp rate  $\eta$ , we find that  $\eta = 56.7 \text{ ns}^{-2}$  leads to the fastest reversal for  $T = 10 \text{ K}$ , as shown by the blue line. Thus, we find that the optimal chirp rate is temperature-dependent, which is an issue has to be considered in device applications. For the 4-nm cube, when  $T > 120 \text{ K}$ , the reversal to  $m_z = -0.7$  is no longer valid. We define this highest temperature that the DCMWP-driven reversal is possible as  $T_m$ .  $T_m = 120 \text{ K}$  for the 4-nm cube is not practically useful. To increase  $T_m$  so that it's higher than the room temperature, we try to enlarge the volume of the sample. Because the anisotropy energy that stabilize  $\mathbf{m}$  towards the north and south poles is  $E_a = KV$  which is proportional to the volume but the thermal energy  $E_t = k_B T$  is independent of the volume [43, 44, 45, 46, 47], increasing the sample volume helps enhancing the stability so that  $T_m$  may be higher. We study  $a = 2, 4, 8, 12 \text{ nm}$  cubic samples, simulate the DCMWP-driven dynamics at different chirp rates, and find the optimal chirp rates for different temperatures. Figure 2(b) shows the optimal chirp rates  $\eta$  (in a step size of  $4.2 \text{ ns}^{-2}$ ) as the function of temperature for different sam-

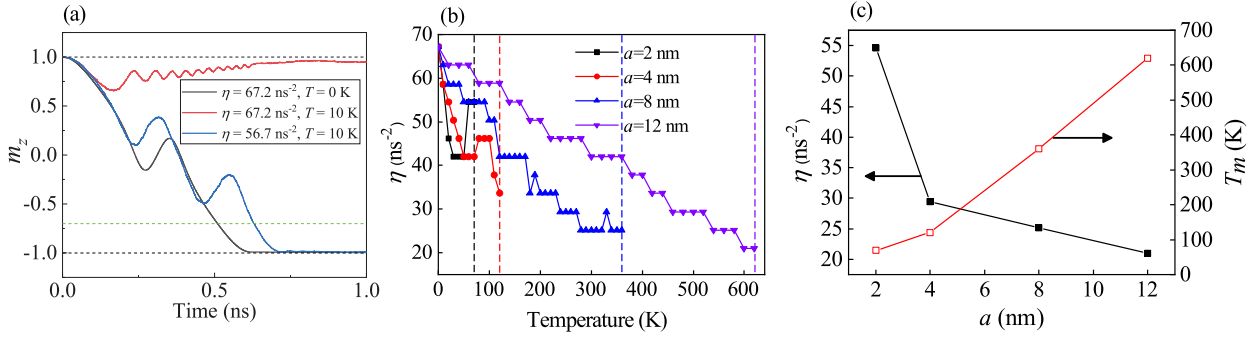


**Figure 2:** (a) The time evolution of  $m_z$  of  $a = 4 \text{ nm}$  driven by the DCMWP with  $f_0 = 21 \text{ GHz}$ ,  $H_{\text{mw}} = 0.045 \text{ T}$  and optimal chirp rates  $\eta$  for different  $T$ . (b) Optimal chirp rate  $\eta$  as a function of  $T$  for different cubic nanoparticles edge length  $a$ . (c) Estimated optimal chirp rate  $\eta$  (solid squares) and maximal temperature  $T_m$  (open squares) are the function of  $a$ .

ple sizes.  $\eta$  shows an overall decreasing trend with increasing temperature, despite some fluctuations which may be due to the complex dynamics induced by the stochastic field and chirp field. The vertical dashed line is the maximal temperature  $T_m$  for each size, which increases with the sample size. For the 12-nm sample,  $T_m$  is above room temperature which means DCMWP-driven magnetization reversal is possible at room temperature and useful in device applications. To be more explicit, we plot  $T_m$  and the optimal chirp rate at  $T_m$  [ $\eta(T_m)$ ] versus the sample volume  $V = a^3$ . As expected, the  $T_m$  increases with  $V$ , while  $\eta(T_m)$  decreases with  $V$ . Since the reversal time is closed to the pulse duration  $\tau = \frac{2f_0}{\eta}$ , the reversal time increases with the temperature, as shown in the Fig. 2(c).

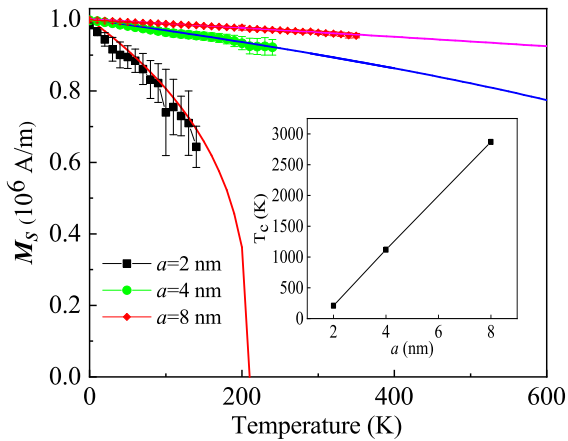


**Figure 3:**  $M_s$  is a function of  $T$  for different cubic nanoparticles edge,  $a$ . Inset shows the Curie temperature,  $T_c$  as a function of the edge length,  $a$ .

To understand the reason why the optimal chirp rate decreases with temperature, we recall the basic knowledge that the effective saturation magnetization  $M_s$  decreases with temperature due to the spin-wave excitation [52]. We numerically calculate the temperature dependence of saturation magnetization  $M_s$  by taking a long-time average of  $M_z$  without

any external driving forces. It is found that  $M_s$  decreases with  $T$  rapidly for smaller volume but decreases slowly for larger volume. The  $M_s - T$  relation can be well fitted by the well-known power law  $M_s(T) = M_s(0) \times (1 - \frac{T}{T_c})^{1/3}$  where  $T_c$  is the Curie temperature. By extrapolating the  $M_s - T$  curves to  $M_s = 0$ , we estimated the Curie temperature, as shown in the insets of the Fig. 3. The Curie temperature increases with the volume as expected. The reduced effective  $M_s$  leads to a reduced intrinsic characteristic frequency  $\gamma M_s$ . Consequently, all the dynamics slow down (as if the time scale of the dynamics is “expanded”) and the reversal time as well as the inverse of chirp rate increases correspondingly.

Due to the reduced effective  $M_s$  and “expanded” time, we can expect that the optimal initial frequency  $f_0$  should also decrease with temperature. Purposely, by keeping the microwave amplitude  $H_{\text{mw}} = 0.045 \text{ T}$  and the optimal chirp rate  $\eta$  at corresponding temperature fixed, we examine the temperature effect on  $f_0$  of DCMWP for the sample  $a = 4 \text{ nm}$  cube. It is observed that the minimal  $f_0$  decreases with temperature  $T$  is shown by red line in the Fig. 4 (a). For the 4-nm cubic sample, the minimal  $f_0$  is 20.3 GHz at the maximal temperature which is still far below the room temperature. To reduce  $f_0$  and increase  $T_m$  further, we study the magnetization reversal with enlarging the sample volume. Fig. 4 (a) shows that the minimal  $f_0$  decreases with  $T$  as well as sample volume which is consistent with the reduction of effective  $M_s$ . For smaller sample,  $f_0$  decreases with  $T$  rapidly but for larger volume, decreases slowly. The vertical dashed lines indicate the minimal  $f_0$  at  $T_m$ . To be more explicit, the minimal  $f_0$  at  $T_m$  i.e., [ $f_0(T_m)$ ] and  $T_m$  are plotted as a function of the sample volume. The minimal  $f_0$  at  $T_m$  decreases (black line) but  $T_m$  increases (red line) with the sample volume shown in Fig. 4(b). Specifically, for 12-nm sample at above the room temperature  $T_m = 320 \text{ K}$ , with  $\eta = 42 \text{ ns}^{-2}$  and  $H_{\text{mw}} = 0.045 \text{ T}$ ,  $f_0$  significantly reduces to 18 GHz.

Later on, by keeping the  $f_0 = 21 \text{ GHz}$  and the optimal chirp rate  $\eta$  at corresponding  $T$  fixed, we investigate the tem-

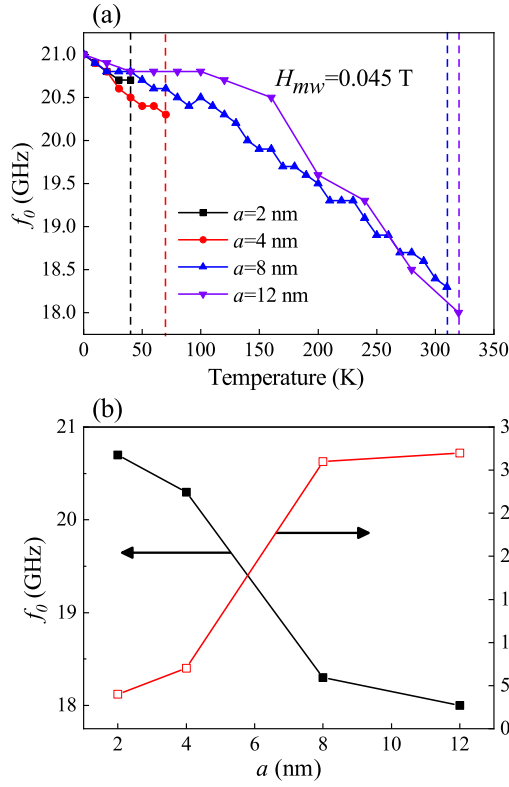


**Figure 4:** (a) Temperature  $T$  dependence of  $f_0$  while  $H_{mw} = 0.045$  T and the optimal  $\eta$  at corresponding  $T$  are fixed. (b) The minimal  $f_0$  (solid squares) at  $T_m$  and the maximal temperature  $T_m$  (open squares) as the function of the edge length  $a$ .

perature dependence of the minimally  $H_{mw}$  of DCMWP required for different sample volumes (2 nm, 4 nm, 8 nm and 12 nm). In this case we also found that the minimal  $H_{mw}$  decreases with the temperature  $T$ , as shown in Fig. 5(a). This is because the finite temperature provides an isotropic background energy which assists the magnetization reversal. Similarly,  $H_{mw}$  decreases with  $T$  up to a maximal temperature  $T_m$ , indicated by vertical dashed lines. Figure 5(b) demonstrates explicitly how the maximal working temperature  $T_m$  and the minimal  $H_{mw}$  at  $T_m$  [ $H_{mw}(T_m)$ ] depend on the sample size. decreases (black line)  $T_m$  increases (red symbols, right axis) and  $H_{mw}(T_m)$  (black symbols, left axis) decreases with the sample size.

Therefore, for 12-nm (or larger) cubic sample, the working temperature can be higher than room temperature, which is practically meaningful. So we search the full parameter space of the DCMWP to find optimal parameters at room temperature:  $H_{mw} \sim 0.038$  T,  $f_0 \sim 19$  GHz and  $\eta \sim 38$  ns<sup>-2</sup>, which gives a fast magnetization reversal time 2 ns. For device applications, one can simulate the reversal dynamics for an actual nano-particle and find the optimal parameters, then this set of parameters can be fixed and used for all the same nano-particles.

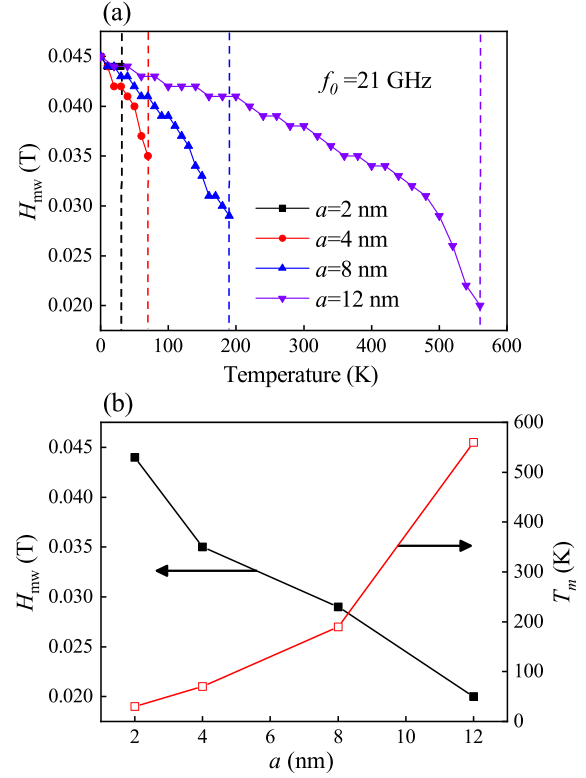


**Figure 5:** (a) Temperature  $T$  dependence of  $H_{mw}$  while  $f_0 = 21$  GHz and the optimal  $\eta$  at corresponding  $T$  are fixed. (b) The minimal  $H_{mw}$  (solid squares) at  $T_m$  and the maximal temperature  $T_m$  (open squares) as a function of the cubic edge  $a$ .

## 4. Discussion and Conclusions

With zero temperature [42], DCMWP-driven subnanosecond magnetization reversal has been demonstrated in zero-temperature limit [42]. In this study, finite temperature effects are included, and the DCMWP-driven fast magnetization reversal is still valid. Since the temperature effectively reduces the energy barrier and expands the time scale, the optimal chirp rate, the optimal initial frequency and the minimal field amplitude decrease with temperature. For the same reason, when the temperature is too high, the magnetization loses its stability, so there is a maximal working temperature for the DCMWP-driven regime. The maximal working temperature can be raised by enlarging the sample volume. In our simulations, 12-nm cubic sample has a maximal working temperature of 320 K, which is slightly higher than the room temperature, indicating that the DCMWP-driven magnetization reversal is practically possible at room temperature for nano-particles larger than  $12^3$  nm<sup>3</sup>. For the 12-nm sample, we find a set of optimal parameters at room temperature, i.e.,  $H_{mw} \sim 0.038$  T,  $f_0 \sim 19$  GHz and  $\eta \sim 38$  ns<sup>-2</sup> which are useful in device application. Since the macrospin model is valid up to 30-nm-diameter nano-particles [46], it is expected that our proposal works for larger nano-particles practically. There are the recent technologies [53, 54] to generate the required microwave chirp pulse. There-

fore, these findings may provide a way to realize low-cost and fast magnetization reversal with a wide operating temperature.

## 5. Acknowledgements

This work was supported by the Khulna University Research Cell (Grant No. KU/RC-04/2000-232). X. S. W. acknowledges the support from the Natural Science Foundation of China (NSFC) (Grant No. 11804045).

## References

- [1] S. Sun, C. B. Murray, D. Weller, L. Folks, A. Moser, Monodisperse fept nanoparticles and ferromagnetic fept nanocrystal superlattices, *science* 287 (5460) (2000) 1989–1992.
- [2] S. Woods, J. Kirtley, S. Sun, R. Koch, Direct investigation of superparamagnetism in co nanoparticle films, *Physical review letters* 87 (13) (2001) 137205.
- [3] D. Zitoun, M. Respaud, M.-C. Fromen, M. J. Casanove, P. Lecante, C. Amiens, B. Chaudret, Magnetic enhancement in nanoscale corh particles, *Physical review letters* 89 (3) (2002) 037203.
- [4] B. Hillebrands, K. Ounadjela, *Spin dynamics in confined magnetic structures I & II*, Vol. 83, Springer Science & Business Media, 2003.
- [5] S. Mangin, D. Ravelosona, J. Katine, M. Carey, B. Terris, E. E. Fullerton, Current-induced magnetization reversal in nanopillars with perpendicular anisotropy, *Nature materials* 5 (3) (2006) 210–215.
- [6] A. Hubert, R. Schafer, *magnetic domains: the analysis of magnetic microstructures* (1998).
- [7] Z. Sun, X. Wang, Fast magnetization switching of stoner particles: A nonlinear dynamics picture, *Physical Review B* 71 (17) (2005) 174430.
- [8] J. C. Slonczewski, et al., Current-driven excitation of magnetic multilayers, *Journal of Magnetism and Magnetic Materials* 159 (1) (1996) L1.
- [9] L. Berger, Emission of spin waves by a magnetic multilayer traversed by a current, *Physical Review B* 54 (13) (1996) 9353.
- [10] M. Tsoi, A. Jansen, J. Bass, W.-C. Chiang, M. Seck, V. Tsoi, P. Wyder, Excitation of a magnetic multilayer by an electric current, *Physical Review Letters* 80 (19) (1998) 4281.
- [11] J. A. Katine, F. J. Albert, R. A. Buhrman, E. B. Myers, D. C. Ralph, Current-driven magnetization reversal and spin-wave excitations in co/cu/cu pillars, *Phys. Rev. Lett.* 84 (2000) 3149–3152.
- [12] X. Waintal, E. B. Myers, P. W. Brouwer, D. C. Ralph, Role of spin-dependent interface scattering in generating current-induced torques in magnetic multilayers, *Phys. Rev. B* 62 (2000) 12317–12327.
- [13] J. Z. Sun, Spin-current interaction with a monodomain magnetic body: A model study, *Physical Review B* 62 (1) (2000) 570.
- [14] J. Sun, Spintronics gets a magnetic flute, *Nature* 425 (6956) (2003) 359–360.
- [15] M. D. Stiles, A. Zangwill, Anatomy of spin-transfer torque, *Physical Review B* 66 (1) (2002) 014407.
- [16] Y. B. Bazaliy, B. Jones, S.-C. Zhang, Current-induced magnetization switching in small domains of different anisotropies, *Physical Review B* 69 (9) (2004) 094421.
- [17] R. Koch, J. Katine, J. Sun, Time-resolved reversal of spin-transfer switching in a nanomagnet, *Physical review letters* 92 (8) (2004) 088302.
- [18] W. Wetzels, G. E. Bauer, O. N. Jouravlev, Efficient magnetization reversal with noisy currents, *Physical review letters* 96 (12) (2006) 127203.
- [19] A. Manchon, S. Zhang, Theory of nonequilibrium intrinsic spin torque in a single nanomagnet, *Physical Review B* 78 (21) (2008) 212405.
- [20] I. M. Miron, G. Gaudin, S. Auffret, B. Rodmacq, A. Schuhl, S. Pizzini, J. Vogel, P. Gambardella, Current-driven spin torque induced by the rashba effect in a ferromagnetic metal layer, *Nature materials* 9 (3) (2010) 230–234.
- [21] I. M. Miron, K. Garello, G. Gaudin, P.-J. Zermatten, M. V. Costache, S. Auffret, S. Bandiera, B. Rodmacq, A. Schuhl, P. Gambardella, Perpendicular switching of a single ferromagnetic layer induced by in-plane current injection, *Nature* 476 (7359) (2011) 189–193.
- [22] L. Liu, C.-F. Pai, Y. Li, H. Tseng, D. Ralph, R. Buhrman, Spin-torque switching with the giant spin hall effect of tantalum, *Science* 336 (6081) (2012) 555–558.
- [23] J. Grollier, V. Cros, H. Jaffres, A. Hamzic, J.-M. George, G. Faini, J. B. Youssef, H. Le Gall, A. Fert, Field dependence of magnetization reversal by spin transfer, *Physical Review B* 67 (17) (2003) 174402.
- [24] H. Morise, S. Nakamura, Stable magnetization states under a spin-polarized current and a magnetic field, *Physical Review B* 71 (1) (2005) 014439.
- [25] T. Taniguchi, H. Imamura, Critical current of spin-transfer-torque-driven magnetization dynamics in magnetic multilayers, *Physical Review B* 78 (22) (2008) 224421.
- [26] Y. Suzuki, A. A. Tulapurkar, C. Chappert, Spin-injection phenomena and applications, in: *Nanomagnetism and Spintronics*, Elsevier, 2009, pp. 93–153.
- [27] Z. Sun, X. Wang, Theoretical limit of the minimal magnetization switching field and the optimal field pulse for stoner particles, *Physical review letters* 97 (7) (2006) 077205.
- [28] X. Wang, Z. Sun, Theoretical limit in the magnetization reversal of stoner particles, *Physical review letters* 98 (7) (2007) 077201.
- [29] X. Wang, P. Yan, J. Lu, C. He, Euler equation of the optimal trajectory for the fastest magnetization reversal of nano-magnetic structures, *EPL (Europhysics Letters)* 84 (2) (2008) 27008.
- [30] G. Bertotti, C. Serpico, I. D. Mayergoyz, Nonlinear magnetization dynamics under circularly polarized field, *Physical Review Letters* 86 (4) (2001) 724.
- [31] Z. Sun, X. Wang, Strategy to reduce minimal magnetization switching field for stoner particles, *Physical Review B* 73 (9) (2006) 092416.
- [32] S. I. Denisov, T. V. Lyuty, P. Hänggi, K. N. Trohidou, Dynamical and thermal effects in nanoparticle systems driven by a rotating magnetic field, *Physical Review B* 74 (10) (2006) 104406.
- [33] S. Okamoto, N. Kikuchi, O. Kitakami, Magnetization switching behavior with microwave assistance, *Applied Physics Letters* 93 (10) (2008) 102506.
- [34] J.-G. Zhu, Y. Wang, Microwave assisted magnetic recording utilizing perpendicular spin torque oscillator with switchable perpendicular electrodes, *IEEE Transactions on Magnetics* 46 (3) (2010) 751–757.
- [35] C. Thirion, W. Wernsdorfer, D. Mailly, Switching of magnetization by nonlinear resonance studied in single nanoparticles, *Nature materials* 2 (8) (2003) 524–527.
- [36] K. Rivkin, J. B. Ketterson, Magnetization reversal in the anisotropy-dominated regime using time-dependent magnetic fields, *Applied physics letters* 89 (25) (2006) 252507.
- [37] Z. Wang, M. Wu, Chirped-microwave assisted magnetization reversal, *Journal of Applied Physics* 105 (9) (2009) 093903.
- [38] N. Barros, M. Rassam, H. Jirari, H. Kachkachi, Optimal switching of a nanomagnet assisted by microwaves, *Physical Review B* 83 (14) (2011) 144418.
- [39] N. Barros, H. Rassam, H. Kachkachi, Microwave-assisted switching of a nanomagnet: Analytical determination of the optimal microwave field, *Physical Review B* 88 (1) (2013) 014421.
- [40] T. Tanaka, Y. Otsuka, Y. Furomoto, K. Matsuyama, Y. Nozaki, Selective magnetization switching with microwave assistance for three-dimensional magnetic recording, *Journal of Applied Physics* 113 (14) (2013) 143908.
- [41] G. Klughertz, P.-A. Hervieux, G. Manfredi, Autoresonant control of the magnetization switching in single-domain nanoparticles, *Journal of Physics D: Applied Physics* 47 (34) (2014) 345004.
- [42] M. T. Islam, X. Wang, Y. Zhang, X. Wang, Subnanosecond magnetization reversal of a magnetic nanoparticle driven by a chirp microwave field pulse, *Physical Review B* 97 (22) (2018) 224412.
- [43] R. H. Koch, G. Grinstein, G. Keefe, Y. Lu, P. Trouilloud, W. Gal-

- lagher, S. Parkin, Thermally assisted magnetization reversal in submicron-sized magnetic thin films, *Physical review letters* 84 (23) (2000) 5419.
- [44] Z. Li, S. Zhang, Thermally assisted magnetization reversal in the presence of a spin-transfer torque, *Physical Review B* 69 (13) (2004) 134416.
- [45] J. De Vries, T. Bolhuis, L. Abelmann, Temperature dependence of the energy barrier and switching field of sub-micron magnetic islands with perpendicular anisotropy, *New journal of physics* 19 (9) (2017) 093019.
- [46] J. M. Iwata-Harms, G. Jan, H. Liu, S. Serrano-Guisan, J. Zhu, L. Thomas, R.-Y. Tong, V. Sundar, P.-K. Wang, High-temperature thermal stability driven by magnetization dilution in c0feb free layers for spin-transfer-torque magnetic random access memory, *Scientific reports* 8 (1) (2018) 1–7.
- [47] W. Liu, B. Cheng, S. Ren, W. Huang, J. Xie, G. Zhou, H. Qin, J. Hu, Thermally assisted magnetization control and switching of dy3fe5o12 and tb3fe5o12 ferrimagnetic garnet by low density current, *Journal of Magnetism and Magnetic Materials* (2020) 166804.
- [48] T. L. Gilbert, A phenomenological theory of damping in ferromagnetic materials, *IEEE transactions on magnetics* 40 (6) (2004) 3443–3449.
- [49] D. Hinzke, N. Kazantseva, U. Nowak, O. N. Mryasov, P. Asselin, R. W. Chantrell, Domain wall properties of fept: From bloch to linear walls, *Phys. Rev. B* 77 (2008) 094407. doi:10.1103/PhysRevB.77.094407.  
URL <https://link.aps.org/doi/10.1103/PhysRevB.77.094407>
- [50] A. Vansteenkiste, J. Leliaert, M. Dvornik, M. Helsen, F. Garcia-Sanchez, B. Van Waeyenberge, The design and verification of mumax3, *AIP advances* 4 (10) (2014) 107133.
- [51] M. T. Islam, X. Wang, X. Wang, Thermal gradient driven domain wall dynamics, *Journal of Physics: Condensed Matter* 31 (45) (2019) 455701.
- [52] C. Kittel, *Introduction to Solid State Physics*, 8th Edition, Wiley, 2004.  
URL [http://www.amazon.com/Introduction-Solid-Physics-Charles-Kittel/dp/047141526X/ref=dp\\_ob\\_title\\_bk](http://www.amazon.com/Introduction-Solid-Physics-Charles-Kittel/dp/047141526X/ref=dp_ob_title_bk)
- [53] L. Cai, D. A. Garanin, E. M. Chudnovsky, Reversal of magnetization of a single-domain magnetic particle by the ac field of time-dependent frequency, *Physical Review B* 87 (2) (2013) 024418.
- [54] L. Cai, E. M. Chudnovsky, Interaction of a nanomagnet with a weak superconducting link, *Physical Review B* 82 (10) (2010) 104429.